Applied Catalysis B: Environmental 92 (2009) 114–125

Contents lists available at ScienceDirect

Applied Catalysis B: Environmental

journal homepage: www.elsevier.com/locate/apcatb

The alteration of the performance of field-aged Pd-based TWCs towards CO and C_3H_6 oxidation

Iljeong Heo [a], Jin Woo Choung [a,b], Pyung Soon Kim [a], In-Sik Nam [a,*], Young Il Song [b], Chi Bum In [b], Gwon Koo Yeo [b,c]

[a] Department of Chemical Engineering/School of Environmental Science and Engineering, Pohang University of Science and Technology (POSTECH), San 31 Hyoja-Dong, Pohang 790-784, Republic of Korea
[b] Exhaust Emission Engineering Team, Power Train R&D Center, Hyundai-Kia Motors Company, Jangduk-Dong Hwaseong 445-706, Republic of Korea
[c] Technical Center, Ordeg Corporation, Moknae-Dong, Ansan 425-100, Republic of Korea

ARTICLE INFO

Article history:
Received 6 May 2009
Received in revised form 13 July 2009
Accepted 20 July 2009
Available online 25 July 2009

Keywords:
TWC
Catalyst deactivation
Cerium-zirconium mixed oxide
OSC
Pd-Ce interaction
Pd sintering
Poisoning

ABSTRACT

The deactivation of a three-way catalyst (TWC) included in warm-up catalytic converters (WCC) employed in passenger vehicles has been examined with respect to the catalyst field mileage by drivers. By a sweep test (ST) under the A/F oscillation of 1 Hz simulating the actual operation of a gasoline engine, the gradual deactivation of CO oxidation activity under rich condition over the Pd TWCs customer-aged was clearly observed with respect to the catalyst mileage, while the oxidation activity of C_3H_6 had been hardly altered. No proportional dependence of the deactivation of the CO and C_3H_6 oxidation activity on the catalyst mileage, however, was determined by both a steady-state sweep test (st-ST) and a light-off test (LOT) without A/F perturbation, although the initial deactivation of both reactions by both test modes was apparent. The sintering of noble metal (NM) itself might not be the only cause for the deactivation of TWC with respect to the catalyst aging mileage. The gradual alteration of the oxygen storage capacity (OSC) of TWC, mainly due to the degradation of the oxygen storage components and the weakness of the Pd-Ce interaction, is also the cause for TWC deactivation, particularly for the CO oxidation reaction under rich condition. No deactivation of the oxidation reaction of C_3H_6 by ST, regardless of the catalyst mileages is likely due to the strong oxidative capability of Pd toward hydrocarbons.

1. Introduction

Since a commercial three-way catalyst (TWC) was developed to reduce the air pollutants emitted from gasoline engine in the 1970s, a catalytic converter containing TWC has been widely employed in the exhaust system of gasoline engines [1,2]. With emission standards becoming more stringent, the performance and configuration of the converter have been significantly improved to meet the ever-tightening emission regulations and market demands. Currently, two converters, including the warm-up and under-flow catalytic converters (WCC and UCC), are independently or simultaneously employed.

WCC, located near the engine mainly for reducing hydrocarbon emissions during the cold-start period, contains two bricks of the TWC monoliths. Since WCC is commonly operated at considerably high exhaust gas temperature due to its location in the exhaust system, the catalysts are easily inactivated by sintering of noble metals (NM) as well as poisoning with lead (Pb), calcium (Ca), zinc (Zn), iron (Fe), phosphorus (P) and sulfur (S) originating from engine lubricants and the gasoline employed [3–8].

Granados et al. claimed that the alteration of the redox property and OSC of TWC aged by customers was not a major cause for the gradual deactivation of the catalyst with respect to the aging mileage, 27,000 and 41,000 miles [9]. No gradual changes of CO and C_3H_6 oxidation activities with respect to the catalyst mileages had been basically observed by LOT with the oscillation of A/F feed ratio, although an apparent initial deactivation was observed in the early stage of the catalyst mileage. In addition, the influence of phosphorus (P) on the catalyst deactivation had hardly been determined with respect to the catalyst mileage.

Moreover, González-Velasco et al. reported the deactivation of CO and C_3H_6 oxidation reactions over Rh, Pd, Pt (Pd-Pt)/Al_2O_3 catalysts containing ceria by ST [10]. No crucial alteration of CO and C_3H_6 oxidation activities over the Pd catalyst upon aging in a muffle furnace at 1173 K for 5 h has been observed, regardless of the A/F ratios ranging from 14.1 to 15.1. Since the catalyst was independently aged, no effect of poisoning by P and S on the catalyst deactivation could be anticipated.

* Corresponding author. Tel.: +82 54 279 2264; fax: +82 54 279 8299.
E-mail address: isnam@postech.ac.kr (I.-S. Nam).

0926-3373/$ – see front matter © 2009 Elsevier B.V. All rights reserved.
doi:10.1016/j.apcatb.2009.07.016

Ceria has been commonly employed for the current TWC system as a promoter for its ability to store and release oxygen, referred to as OSC. Since the OSC enhances the TWC performance, no doubt the role of ceria for reducing the emissions of air pollutants from gasoline engine can be argued [2].

Cerium-zirconium mixed oxides (CZ;$Ce_xZr_{(1-x)}O_2$) have been recently used to moderate the deactivation of TWC besides ceria itself [11,12]. However, CZ is also inactivated by the thermal degradation and poisoning of TWC under the vehicle-aging condition. Moreover, the interaction of the NMs with Ce sharing O atom can be altered, mainly due to the growth of Pd particles by sintering [13,14]. The OSC and catalytic activity of TWC then decrease as the catalyst deactivation proceeds. In addition, the disappearance of the active metal components on the catalyst surface by the encapsulation with alumina and ceria further reduces the OSC of TWC [2,15].

In the present study, the fresh and customer-aged Pd TWCs contained in both WCC only and WCC + UCC systems have been examined to identify the cause for the catalyst deactivation with respect to the catalyst field mileage. The alteration of the oxidation activity of CO and C_3H_6 over the TWCs aged under vehicle condition by customers, not by engine dynamometer has been examined by three TWC test modes including ST with A/F oscillation, st-ST and LOT. The cause for the deactivation of the oxidation reaction over TWC will be clearly determined with respect to the catalyst mileage.

2. Experimental

2.1. Catalyst preparation

Four sets of the customer-aged TWCs contained in WCC only and WCC + UCC systems were provided by Hyundai Motor Company. Among them, Pd-based TWCs located in the front brick were employed for particularly examining the oxidation activity of the catalyst. They are 21,000 and 55,000 mile customer-aged Pd catalysts from the WCC only system, and 41,000 and 98,000 mile aged catalysts from the WCC + UCC system. Note that TWCs contained in each converter system were installed into an identical vehicle model and no other noble metals were included in TWCs besides Pd.

Each section of a whole monolith brick divided into five pieces with respect to the monolith length was ground with its cordierite, or the washcoat layer on the channels of the monolith sectioned was scraped off for properly characterizing TWC. The powder type catalyst obtained from the first piece of each brick sectioned was particularly examined in order to clearly determine the alteration of the activity and characteristics of TWC upon aging with respect to the catalyst mileage, unless specified. The samples were individually designated with respect to the aging mileage. For the Pd7-21,000, "Pd7" stands for the content of Pd per volume of the monolith (g_{Pd}/L), and 21,000 is the catalyst mileage actually driven by the customer.

2.2. Reactor system and experimental procedure

The performance of TWCs was evaluated under three test modes, sweep test (ST), steady-state sweep test (st-ST) and light-off test (LOT), over a fixed bed continuous flow reactor system as illustrated in Fig. 1. 1 g of the powder form of TWC with cordierite ground into 20/30 mesh to minimize the mass transfer limitations was charged into a 3/8 in. U-type stainless steel tube reactor submerged in a molten-salt bath to ensure the isothermal condition of the catalyst bed. The temperature difference of the top and bottom thermocouples installed into the reactor system employed was controlled within 2 K in order to keep the

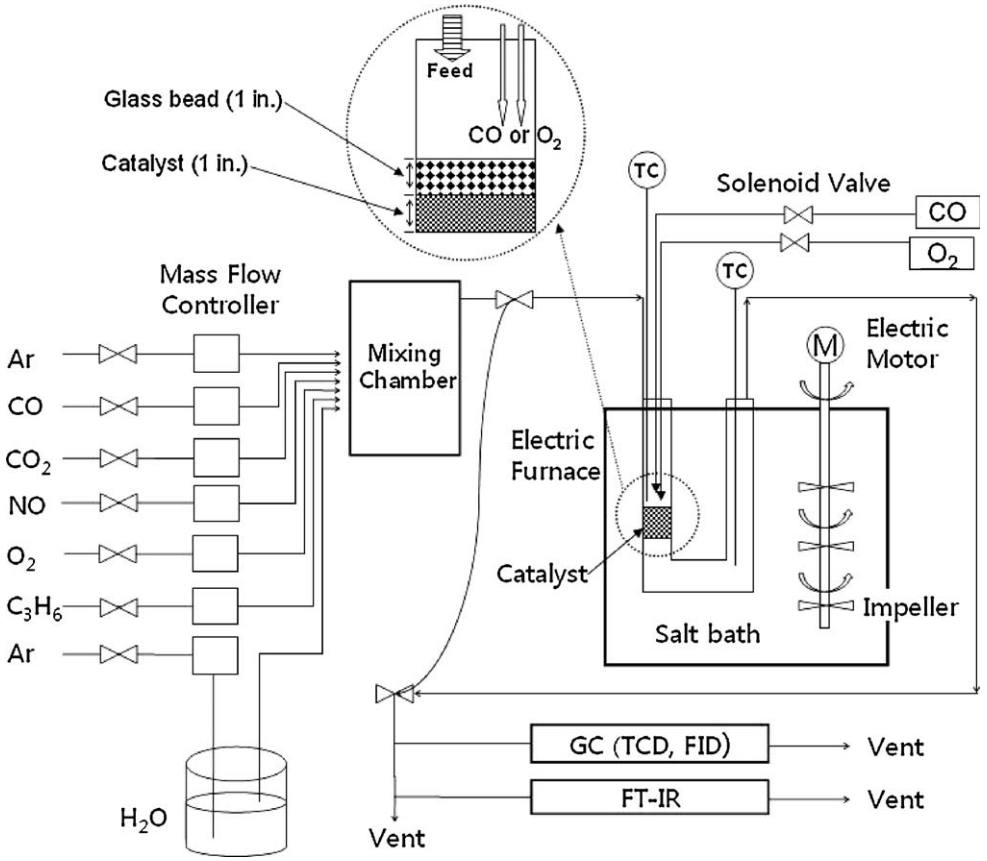

Fig. 1. Schematic flow diagram of the TWC reaction system. The inset in the circle shows the detailed injection part of an additional CO and O_2 for realizing 0.5 A/F and 1 Hz perturbation.

isothermal reaction condition of the catalyst bed. No mixing problem was specifically encountered during the course of the ST by varying the amount of extra CO and O_2 added into the feed gas stream. Indeed, 1 in. thickness of the bed of the glass beads packed into the reactor system in order to improve the mixing and the even distribution of the CO and O_2 injected to the primary feed gas stream as depicted in an inset of Fig. 1, works properly. The concentrations of the inlet and outlet gas compositions were analyzed by on-line gas chromatography (GC) equipped with the TCD and FID (Agilent, Model 6890N) and FT-IR (Thermo Electron Co. Nicolet 5700). Details of the reactor system and experimental procedure are also given elsewhere [10,16,17].

The ST was conducted at 673 K to ensure the deactivation of the oxidation activity of TWC with respect to the catalyst mileage under the normal warm-up operating condition of gasoline engine [1,18,19]. The catalyst was pretreated prior to each experiment under stoichiometric feed condition where air to fuel ratio (A/F) was 14.63 (λ = 1.0) [20]. The conversions of CO and C_3H_6 were then measured with respect to the feed gas condition: λ from 0.97 to 1.03 by changing the O_2 feed concentration from 0.4% to 1.4% with the oscillation of $\pm$0.5 A/F with 1.0 Hz by injecting additional O_2 and CO into feed. The composition of feed gas stream was 1% CO, 500 ppm C_3H_6, 0.4–1.4% O_2, 500 ppm NO, 0.3% H_2, 10% H_2O, 10% CO_2, and Ar balance as listed in Table 1. The reactor space velocity, the ratio of the feed gas flow rate to the volume occupied by the catalyst powder charged into the reactor was 100,000 h^{-1}.

The st-ST was carried out with respect to the A/F ratios at 673 K under steady state without any real time dynamic oscillation of the feed gas stream. In the present study, the ST and st-ST experimental programs were simultaneously set up for discriminating the role of CZ (OSC) and NM for the oxidation activity of TWC. The experimental results by the st-ST may simply determine the cause for the deactivation of TWC without the participation of OSC phenomena in the reaction, since no dynamic perturbation of the feed gas stream, lean and rich was performed for the st-ST.

A light-off test program was designed to examine the alteration of the light-off temperature (T_{50}) by the deactivation of TWC under slightly lean condition (λ = 1.01) in order to avoid the experimental difficulty at the stoichiometric point (λ = 1.00) within the range of temperatures from 423 to 673 K [21–23], although it may not be a useful TWC test mode. Note that T_{50} is the temperature where 50% conversion of the gas composition is achieved. However, the direct contribution of Pd as an active reaction site to the TWC performance can be examined by LOT with respect to the reaction temperatures. Note that both st-ST and LOT simply determine the steady-state performance of TWC, mainly the catalytic activity by NM included in TWC without the dynamic action of OSC.

2.3. Catalyst characterization

The BET surface areas of TWCs were measured from N_2 isotherms at 77 K by volumetric methods (Micromeritics, ASAP 2010). The compositions of the elements included in TWC were examined by inductively coupled plasma-optical emission spectroscopy (ICP-Flame-EOP, Spectro Co.) and C/S analysis (LECO SC-32 analyzer). A transmission electron microscope (TEM, JEOL-2100F) equipped with energy dispersive X-ray spectroscopy (EDS, INCA) was used to identify the state of Pd over the fresh and aged TWCs.

The active metal surface areas of the catalysts were evaluated by pulse CO chemisorption method (AutoChem II 2920, Micromeritics). Details are also given elsewhere [24]. It should be noted that the catalysts were pre-reduced at 773 K in pure H_2 for 2 h before CO pulse injection at 308 K in the present study. Oxygen storage capacity (OSC) and oxygen storage capacity complete (OSCC) [25] of TWC, the criteria for examining the mobility and the storage capacity of oxygen over the lattice of CZ, respectively, were also determined at 673 K by using a pulsed 5% H_2/Ar with Autochem II 2920. H_2 temperature-programmed reduction (TPR) experiments were also conducted in a temperature range up to 1173 K with 10 K/min under 5% H_2/Ar flow of 50 ml/min after redox treatment at 673 K [22]. The composition of the downstream from TPR system was monitored by a GC equipped with TCD (5890, Hewlett Packard) and a mass spectrometer (QMI422, Pfeiffer Vacuum).

Synchrotron radiation X-ray diffraction (SR-XRD) of the catalyst samples was determined at the 8C2 beam line in the Pohang Accelerator Laboratory (PAL). The incident X-rays were monochromatized to a wavelength of 1.5453 Å by a double-crystal Si(1 1 1) monochromator. The X-ray absorption near edge structure (XANES) spectra for Ce L_3-edge of the samples at 5723 eV was obtained at the 3C1 beam line of PAL [26]. X-ray photoelectron spectroscopy (XPS) spectra of the catalyst samples were also obtained by using a VG ESCALAB 220i equipped with an Mg anode. The binding energies were corrected by the C 1s line at 284.6 eV. It should be noted that the TWC directly scraped off from the channels of monoliths was employed for TEM, XRD, XANES and XPS, while the catalyst powder with cordierite was used for the rest of the characterization methods.

Table 1
Feed gas compositions for LOT, st-ST and ST.

Components	Concentrations		
	LOT	st-ST	ST (with perturbation)
CO	1%	1%	1% (with 0.46 cm^3 CO)
C_3H_6	500 ppm	500 ppm	500 ppm
O_2	1%	0.4–1.4%	0.4–1.4% (with 0.23 cm^3 O_2)
NO	500 ppm	500 ppm	500 ppm
H_2	0.3%	0.3%	0.3%
H_2O	10%	10%	10%
CO_2	10%	10%	10%
Ar	Balance	Balance	Balance

ST was conducted under A/F perturbation ($\pm$0.5 A/F, 1 Hz).

3. Results

3.1. Effect of the catalyst mileage on the oxidation activity of CO and C_3H_6

Varying λ from 0.97 to 1.03 by controlling the oxygen feed concentration from 0.4% to 1.4% with the perturbation of $\pm$0.5 A/F with 1.0 Hz in order to simulate the actual exhaust composition from gasoline engine, the ST was conducted at 673 K of the normal operating temperature of gasoline engine under warm-up condition [1,18,19].

Fig. 2(a) and (b) present the oxidation activities of CO and C_3H_6 examined by the ST over the fresh, 21,000 and 55,000 mile customer-aged Pd7 TWCs. Under the lean condition where O_2 excessively exists in the feed gas stream, both CO and C_3H_6 are completely oxidized, regardless of the catalyst mileage. However, the CO oxidation activities of the aged TWCs under the rich condition gradually decrease as the catalyst mileage increases, while no change of the C_3H_6 oxidation activities has been observed again, regardless of the catalyst aging mileage. This is mainly due to the dominant oxidative capability of Pd-based catalyst toward C_3H_6 as well as the dynamic action of OSC by CZ at this reaction temperature [17,27–29]. Similar results were also observed over the Pd10 TWCs employed for WCC + UCC system, which were independently used by the area and driver compared to that over the Pd7 TWC contained in the WCC only converter system as discussed. Note that the content of Pd in Pd10 TWC is about 40% higher than that in Pd7 TWC. The deactivation trend of the

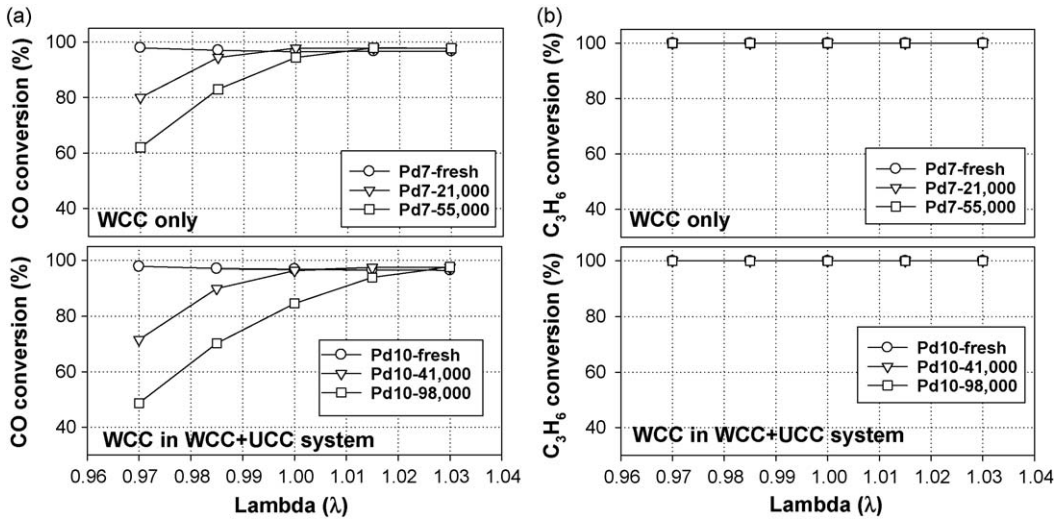

Fig. 2. Oxidation activity of CO and C_3H_6 by the sweep test (ST) over the fresh and aged Pd TWC (front brick of WCC); (a) CO oxidations, and (b) C_3H_6 oxidations of the Pd7 and Pd10 TWCs at 673 K. The Pd7 and Pd10 TWC bricks are contained in WCC only and WCC + UCC converters, respectively.

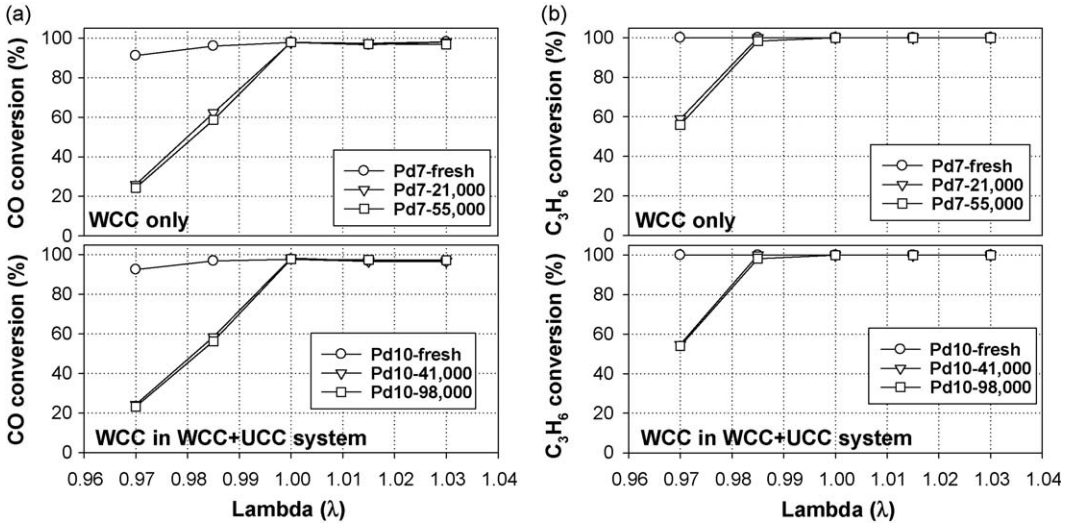

Fig. 3. Oxidation activity of CO and C_3H_6 by the steady-state sweep test (st-ST) over the fresh and aged Pd TWCs; (a) CO oxidations, and (b) C_3H_6 oxidations of the Pd7 and Pd10 TWCs at 673 K.

oxidation activity over TWC by ST is similar, regardless of the Pd content and the operating conditions of vehicles varied by area and operator.

Since the st-ST was conducted under steady state at the given A/F ratio without its dynamic perturbation, no action of the OSC components for uptaking and releasing O_2 onto and from TWC at 673 K can be expected [17,27]. Apparent initial deactivations of TWCs upon aging are observed for both CO and C_3H_6 oxidation reactions under the rich feed condition as shown in Fig. 3(a) and (b). Although no dynamic action of CZ is expected for st-ST, both oxidation reactions reveal an apparent initial deactivation of TWC in an early stage of the catalyst mileage. Once the catalyst, Pd7 TWC was aged for 21,000 miles, no further deactivation was observed up to 55,000 miles of the catalyst mileage. Again, a similar trend was examined over the 41,000 and 98,000 mile aged Pd 10 catalyst employed in the WCC + UCC system.

Fig. 4 shows the results by LOT over the fresh and aged TWCs conducted at $\lambda = 1.01$, slightly lean condition, within the temperature range from 425 to 675 K. By LOT, the role of noble metal for the TWC performance can be maximized, since the test is conducted under slightly excess O_2 condition where no role of CZ for the catalyst OSC can be expected. Similar to the results by st-ST, the deactivation of CO and C_3H_6 oxidation reactions has been observed in the initial period of catalyst aging as shown in Fig. 4. Furthermore, the light-off temperatures (T_{50}) for CO and C_3H_6 reactions hardly shift to the higher temperature region after initial increase, regardless of the catalyst mileage and Pd content. However, the conversion of C_3H_6 below 573 K over Pd10-98,000, the highest catalyst mileage among the catalysts examined in the present study slightly shifts to the higher temperature region. This may be due to another deactivation cause by the disappearance of Pd through severe encapsulation upon the initial sintering of NM [2,15]. It should be noted that no specific change of the trend of TWC performance has been observed with respect to the reactor operating condition, including the reactor space velocity and A/F feed condition and the monolith length.

Compared to that by ST, the trend of the TWC activity confirmed by the st-ST and LOT revealing no gradual deactivation of the CO oxidation reaction with respect to the catalyst mileages is unique. No gradual sintering of the catalyst with respect to the catalyst mileage can be anticipated by st-ST and LOT. In addition, no deactivation of the oxidation activity of C_3H_6 by ST has been

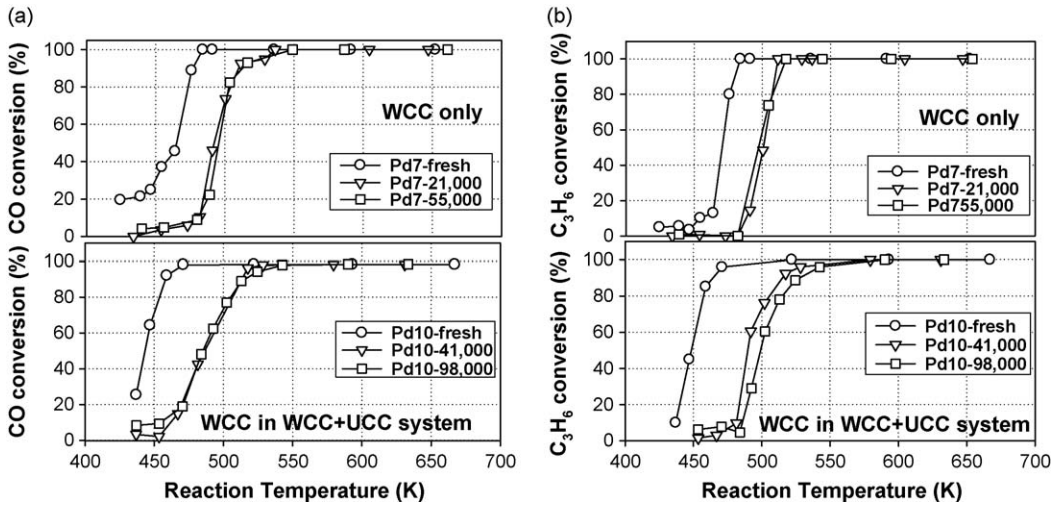

Fig. 4. Oxidation activity of CO and C_3H_6 by the light-off test (LOT) at λ = 1.01 over the fresh and aged Pd TWCs; (a) CO oxidations, and (b) C_3H_6 oxidations of the Pd7 and Pd10 TWCs.

observed, regardless of the feed gas condition, rich and lean, while its initial deactivation by st-ST and LOT is apparent in the early stage of the catalyst mileage.

It is interesting to understand the reason for these distinct deactivation trends of both CO and C_3H_6 oxidation reactions observed by three test modes, ST, st-ST and LOT over Pd TWCs, regardless of the content of Pd of TWCs, Pd7 and Pd10. The dynamic role of OSC may critical for the catalyst deactivation, particularly the oxidation reaction under rich condition. The multiple causes for the deactivation of TWC then can be anticipated. Although the sintering of the NM itself has been commonly regarded as a primary cause for the inactivation of TWC [1,2], the alteration of the OSC of TWC, probably due to the degradation of CZ and/or weakness of Pd-Ce interaction cannot be ignored to identify the cause for the deactivation of the oxidation reactions over TWC with respect to the catalyst aging mileages [30].

Based upon the results by ST, st-ST and LOT, the main cause for the catalyst deactivation of TWCs, particularly Pd contained in the front brick of the converter, is not only the sintering of NM, but also the degradation of the OSC of TWC. In addition, the ST is an essential test mode for appropriately identifying the cause for the deactivation of the oxidation activity of TWC with respect to the catalyst mileages.

3.2. Alteration of physicochemical characteristics of the TWCs field-aged

3.2.1. Sintering of Pd

As reflected in the results by the TWC activity tests, ST, st-ST and LOT conducted in the present study, the cause for the initial deactivation may be attributed to the sintering of NM upon aging. However, the sintering of NM itself cannot properly explain the trend of the gradual deactivation of TWC activity, particularly CO oxidation reaction determined by ST under rich condition with respect to the catalyst mileage. To identify the cause for the deactivation of TWC, the fresh and aged TWCs were examined by a variety of the catalyst characterization techniques. As listed in Table 2, BET surface areas of the TWCs, including cordierite, apparently decrease with respect to the catalyst aging mileage. However, no proportional change of the TWCs' areas with respect to the catalyst mileage has been observed within the error ranges of the measurement based upon the changing degree of the surface areas of TWCs including cordierite. The gradual decrease of the oxidation activities is not mainly due to the decrease of the surface areas of the TWCs employed, while the initial deactivation of the fresh TWC may be related to the decrease of the catalyst surface areas. Note that the cordierite content, approximately 70% in weight included in the catalyst samples employed, hardly affected the decreasing trend of the real surface area of TWC.

Once the catalysts were aged, an apparent initial increase of the Pd particle size and decrease of metallic surface area of Pd by CO chemisorption were identified as listed in Table 2. However, the altered degree of the catalyst characteristics including the diameter of the Pd particles, their dispersions on the catalyst surface, the Pd metallic surface areas and the surface areas of the TWCs, is hardly proportional to that of the catalyst mileage. The sintering of Pd clearly occurs in the initial period of the catalyst aging even over Pd7-21,000, and no further change of the catalyst characteristics including metallic dispersion, surface area and diameter has been observed. It again reveals that the sintering of NM itself may not be the only cause for the deactivation of TWC. Indeed, this may be a reason why the trend of the deactivation of TWC can be hardly elucidated by st-ST and LOT without the dynamic perturbation of A/F in the feed gas stream.

Table 2
Alteration of physical properties of the fresh and aged Pd TWCs.

Samples	BET surface areas (m^2/g)	Active metal *stoichiometry factor = 1		
		Diameters (nm)	Dispersions (%)	Metallic surface areas (m^2/g_{cat})
Pd7-fresh	24	2.6	43.2	1.89
Pd7-21,000	12	35.8	3.1	0.19
Pd7-55,000	10	55.6	2.0	0.12
Pd10-fresh	27	2.6	42.6	2.64
Pd10-41,000	10	71.9	1.6	0.096
Pd10-98,000	8	112.0	1.0	0.062

Fig. 5 shows the XPS spectra of the TWCs in the region of Pd 3d. The fresh Pd catalysts contained in both WCC only and WCC + UCC systems reveal the peaks for Pd $3d_{5/2}$ at 336.3 eV assigned to PdO species formed on the catalyst surface [30]. However, once the TWCs were aged in the vehicle, the peak disappeared and shifted to the binding energy at 334.7 eV to be assigned to the larger Pd particles agglomerated by sintering of Pd metals on the catalyst surface [31,32]. Furthermore, the gradual disappearance of the large Pd particles from the catalyst surface was also observed with respect to the catalyst mileage, regardless of the catalyst Pd content.

Fig. 6 shows the TEM images of the fresh (Pd7-fresh) and the aged (Pd7-55,000) TWC samples. A variety of the elements including Al, Zr, Ce and Pd can be identified by EDS of TEM as shown in Fig. 6 and Table 3. No isolated CeO_2 phase without Zr exists on the surface of the Pd7-fresh catalyst as observed by EDS analysis. It is always with Zr in a form of CZ. The Ce-rich phase on the surface of the Pd7-55,000 however starts to form upon aging [33]. The formation of the larger Pd particles with a size of approximately 60 nm is clearly observed over Pd7-55,000 shown in Fig. 6(b) and (d). It is consistent with the particle size calculated by the CO chemisorption as listed in Table 2.

3.2.2. Poisoning of TWC

The amounts of the contaminants from fuel and lubricants deposited onto the surface of TWC during the course of the vehicle operation were determined by ICP with respect to the catalyst mileages and the length of TWC monolith in Fig. 7. Phosphorus (P) mainly from engine lubricant is the most abundant poison among the contaminants identified in the present study. The content increases and decreases as the catalyst mileage and the monolith length increase, respectively [4,34]. Indeed, the poisoning of Ce by P forming $CePO_4$ on the catalyst surface has been commonly observed over the TWC aged by customers [7,9].

No mileage dependence on the deposition of S mainly from fuel employed was observed. For instance, more S accumulates onto the surface of Pd7-21,000 than Pd7-55,000. Although the total amount of S deposited onto Pd10-41,000 and 98,000 contained in the WCC + UCC system is lower than that onto Pd7 TWCs in the WCC only system, the catalyst mileage of Pd10 TWCs aged is nearly two times longer that of Pd7 TWCs aged. It may be simply due to the operating condition of the engines, including the S content of fuel employed by operators. No apparent deposition of Pb, a well-known deactivation precursor for TWC from fuel additives onto the catalyst surface, is observed [35] with respect to the catalyst mileage, Pd content and monolith length. However, ample amounts of Ca and Zn, mainly from fuel and lubricant, are observed from the surface of TWC with respect to the catalyst mileage and the monolith length.

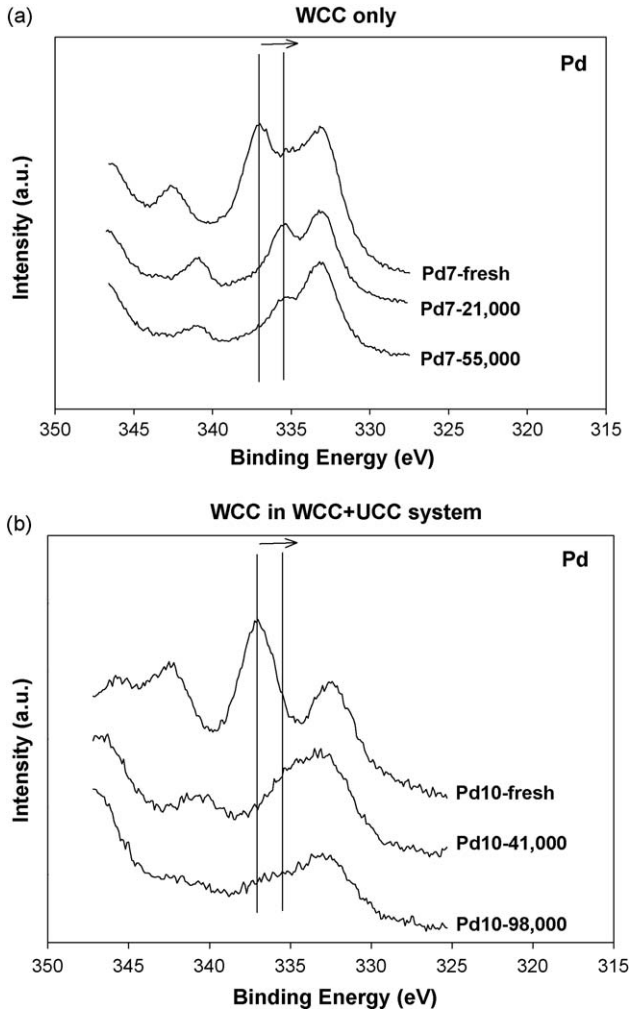

Fig. 5. XPS spectra (Pd 3d) of the fresh and aged Pd TWCs; (a) Pd7 and (b) Pd10 TWCs.

3.2.3. Alteration of CZ

Fig. 8 reveals XRD patterns for the fresh and aged TWCs. CZ ($Ce_xZr_{(1-x)}O_2$) and supplementary ZrO_2 over the fresh TWC as also identified by TEM and EDS analysis included in Fig. 6 and Table 3, exist at around $2\theta = 27–31^\circ$, regardless of the Pd content of the catalyst. In the vicinity of $2\theta = 29.3^\circ$, the broad band assigned to $Ce_{0.5}Zr_{0.5}O_2$ splits into two peaks, CeO_2 ($2\theta = 28.5^\circ$) and ZrO_2 ($2\theta = 29.8^\circ$) due to the phase separation by thermal degradation [36]. Indeed, the formation of the isolated CeO_2 separated from CZ on the surface of Pd7 catalyst upon aging has been identified by TEM and EDS results. The diffraction peak of ZrO_2 at $2\theta = 29.8^\circ$ separated from CZ at $2\theta = 29.3^\circ$ has been overlapped into that of the supplementary ZrO_2 formed on the catalyst surface during the course of the catalyst preparation. Furthermore, the formation of the deactivating agents including $AlPO_4$, $Ca_3(PO_4)_2$, $Ce_2(SO_4)_3{\cdot}5H_2O$ and $CePO_4$ upon the catalyst deactivation was also identified on the catalyst surface [ICDD card, 041-0562, 006-0200, 022-0546 and 026-0355].

The H_2 TPR profiles over the fresh and aged TWCs for WCC only and WCC + UCC systems were examined as shown in Fig. 9. A negative peak due to the decomposition of β hydride type Pd appears at around 348 K [36,37], and a major reduction peak is observed at around 1073 K. The negative peak indicating the presence of the large Pd particles agglomerated by sintering of Pd on the catalyst surface becomes evident upon the catalyst aging, regardless of the catalyst Pd content and mileage [38]. However, the reduction peaks slightly shift to the higher temperature region as the catalyst mileage increases. The peak in the temperature region higher than 900 K is probably attributed to the formation of H_2O and H_2S during the course of TPR, as confirmed by on-line mass spectrometer as shown in the inset of Fig. 9. In addition, the peak at around 600 K observed over Pd10-fresh is mainly attributed to the reduction of NiO added onto TWC to improve its sulfur tolerance [1,39]. The peak shifts to the temperature region higher than 1000 K upon aging by the transformation of NiO to $NiAl_2O_4$ and has been overlapped with that for the bulk phase of CeO_2 [31,39]. Note that no Ni had been added to Pd7 TWC but to Pd10 TWC.

By the sequential re-oxidation of the Pd7-55,000 at 673 K pre-reduced at 1173 K for 10 min, a new hydrogen consumption peak by the reduction of the surface CeO_2 appears at 723 K [31]. It may reveal that the state of CeO_2 poisoned by S was restored by the thermal

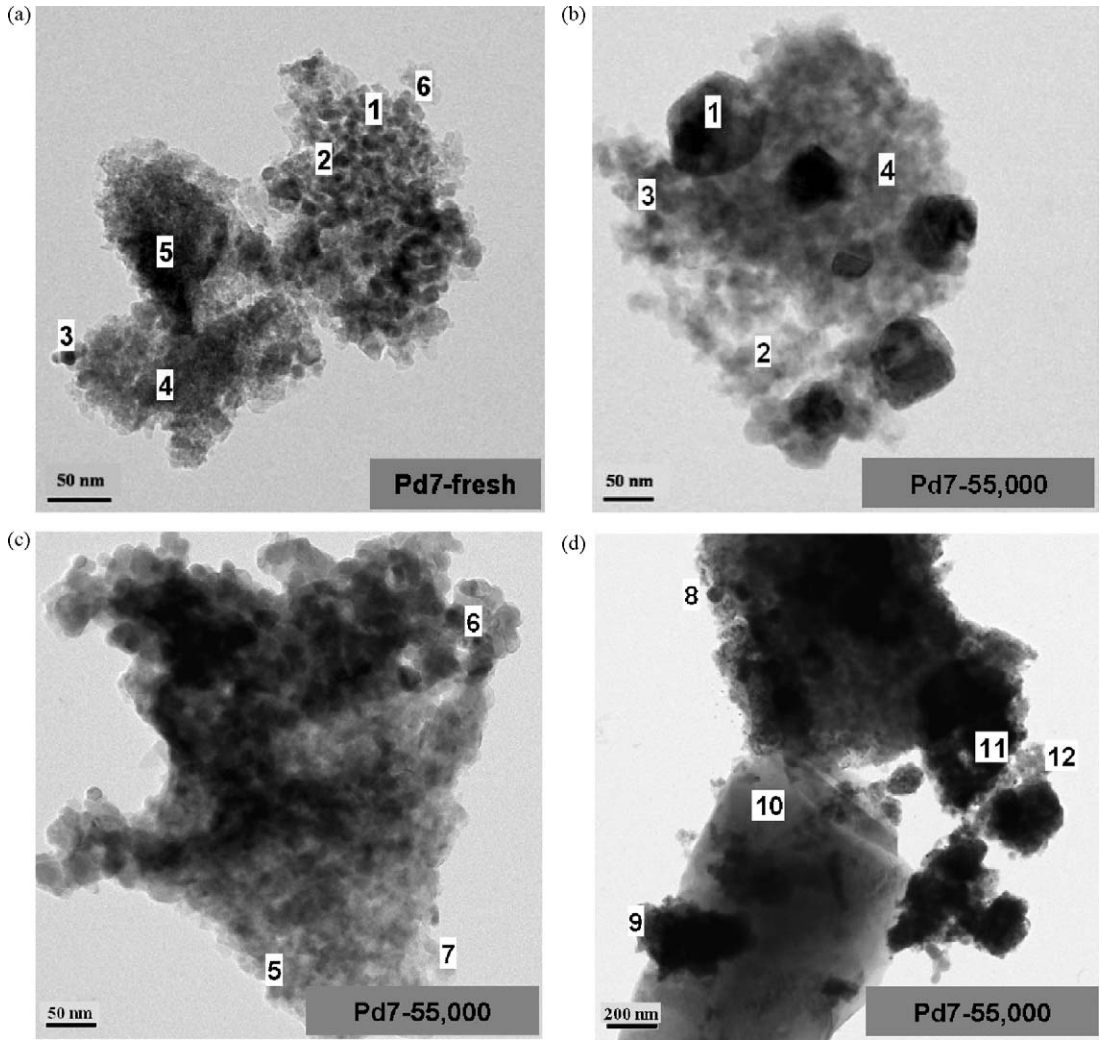

Fig. 6. TEM images of the fresh and aged Pd7 TWC; (a) Pd7-fresh and (b–d) Pd7-55,000.

treatment of aged TWC under reducing condition through the decomposition of $Ce_2(SO_4)_3$ during the course of gasoline engine operation [2,5,40]. In addition, the high temperature reduction peak by bulk CeO_2 at around 1073 K [31,41] previously observed disappears, mainly due to the sequential procedure of TPR.

Fig. 10(a) and (b) are the XANES spectra for Ce L_3-edge for examining the alteration of the oxidation state of Ce species of TWC upon the catalyst aging. Both $Ce(NO_3)_3{\cdot}6H_2O$ and CeO_2 were employed as a reference compound for tri- and tetravalent Ce, respectively. An edge peak of Ce^{3+} compound similar to the XANES peak for $Ce(NO_3)_3{\cdot}6H_2O$ has been observed at 5727 eV (peak B). The formation of three edge peaks to be assigned to Ce^{4+} similar to that by CeO_2 is apparent at 5722 eV (peak A), 5721 (peak C) and 5738 eV (peak D). Although both states of Ce, Ce^{3+} and Ce^{4+} exist on

Table 3
EDS analysis for the catalyst composition over Pd7-fresh and Pd7-55,000.

Components	Pd7-fresh (* atomic %)					
	#1	#2	#3	#4	#5	#6
O	63.38	58.59	62.84	65.80	59.31	52.37
Al	19.94	4.81	1.89	13.88	16.02	43.80
Zr	12.12	31.94	30.58	19.14	13.33	0.25
Pd	0.83	2.2	1.69	0.75	1.59	3.95
Ce	3.52	7.45	4.24	–	10.54	–

Components	Pd7-55,000 (*at.%)											
	#1	#2	#3	#4	#5	#6	#7	#8	#9	#10	#11	#12
O	41.63	49.86	54.42	52.13	59.90	65.73	53.04	33.49	42.27	48.83	57.30	62.75
Al	1.95	43.71	26.98	41.64	16.64	1.86	38.29	18.69	15.69	15.67	3.09	28.75
Zr	–	1.01	16.21	0.99	0.4	19.32	1.13	1.34	19.24	0.01	33.76	1.64
Pd	55.51	0.03	0.02	0.57	0.1	–	0.09	43.48	0.33	–	–	–
Ce	–	0.02	0.16	0.18	7.86	8.00	1.21	–	6.59	0.04	2.79	0.69

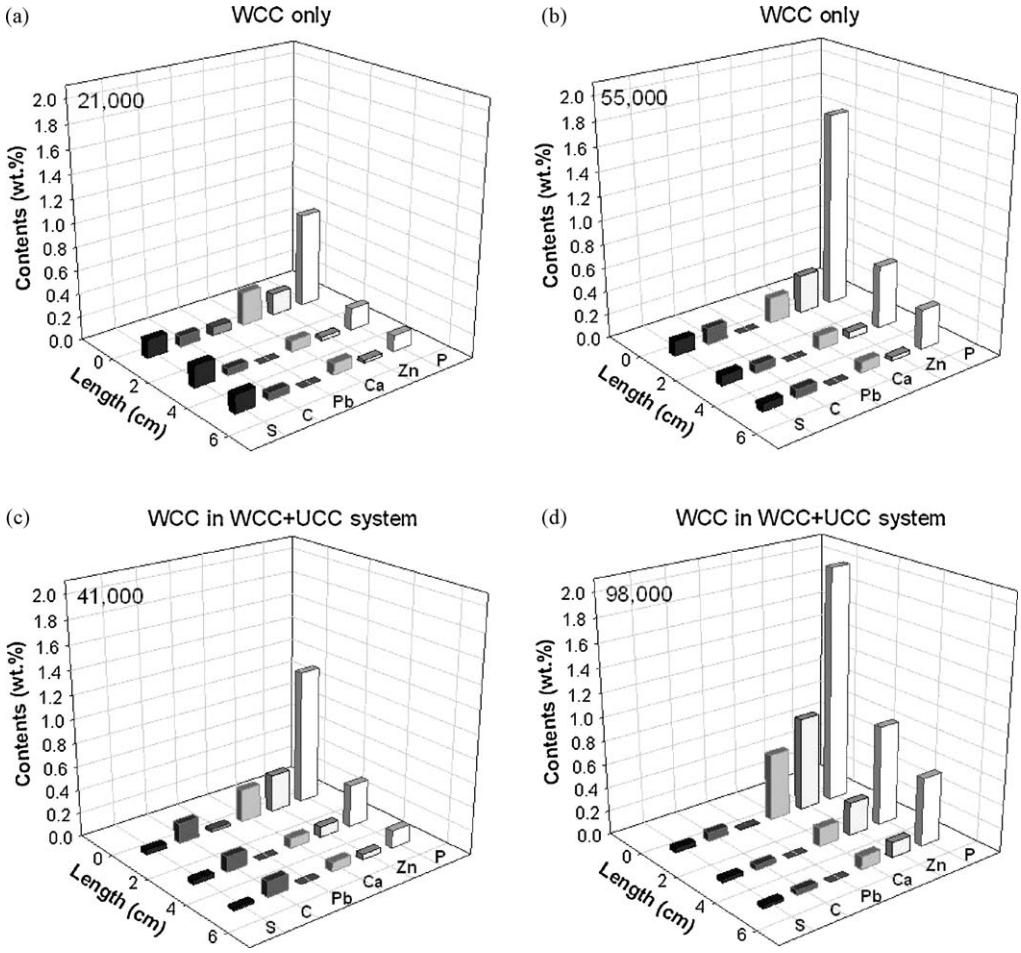

Fig. 7. Composition of the contaminants deposited onto Pd TWCs with respect to the catalyst mileage and the monolith length; (a) and (b) for Pd7, and (c) and (d) for Pd10 TWCs.

the surface of TWC, the intensity of the peak for Ce^{+3} at 5727 eV (peak B) increases as the catalyst aging mileage increases.

Fig. 11(a) and (b) depict the increase of the relative amount of Ce^{3+} contained in CZ upon aging by the deconvolution of the intensity of XANES peak with the arctangent and Gaussian functions [42]. Over both customer-aged TWCs included in WCC only and WCC + UCC systems, the amount of Ce^{3+} existing on the surface of TWCs strongly depends on the catalyst mileage and the catalyst monolith length, regardless of the catalyst Pd content.

The alteration of chemical state of Ce upon the catalyst aging was also identified by XPS as shown in Fig. 12. Two sets of spin-orbit multiplets originating from Ce species on the catalyst surface

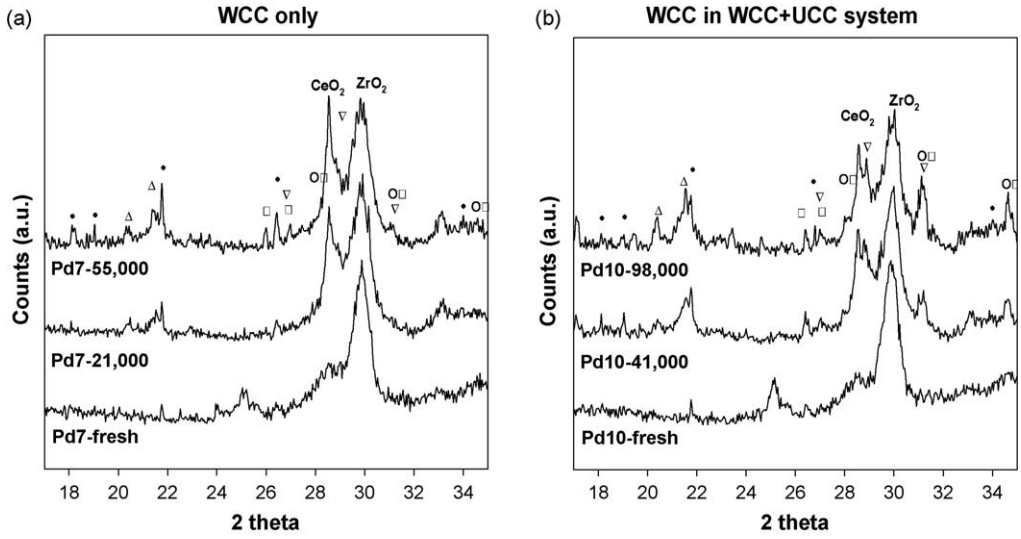

Fig. 8. XRD patterns over the fresh and aged Pd TWCs; (a) Pd7 and (b) Pd10 TWCs. Symbols: (•) cordierite; (△) $AlPO_4$; (□) $Ce_2(SO_4)_3{\cdot}5H_2O$; (▽) $CePO_4$; (○) $Ca_3(PO_4)_2$.

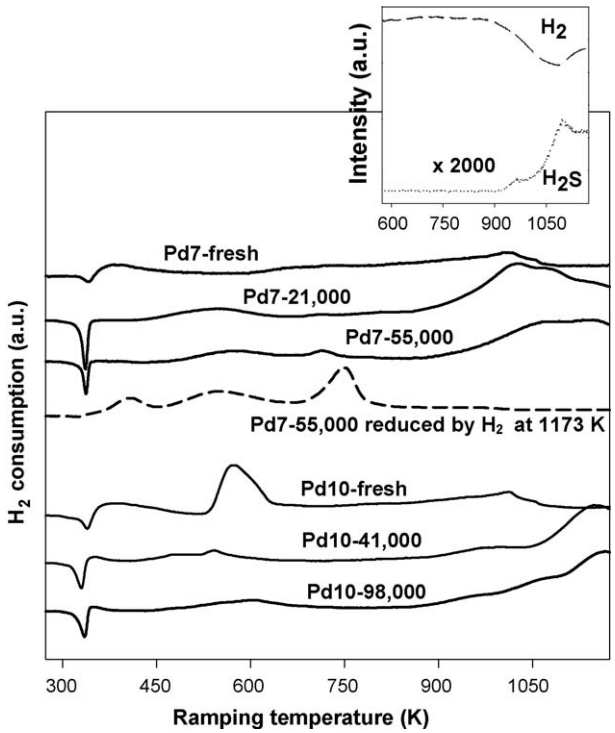

Fig. 9. H_2 TPR profiles over the fresh and aged Pd TWCs; (a) Pd7 TWCs and (b) Pd10 TWCs. The inset shows the decomposition of sulfur compound as H_2S from Pd7-55,000 during H_2 TPR identified by Q-mass spectrometer.

were observed. The peaks are attributed to $3d_{3/2}$ of Ce identified by v, v′, v″ and v‴ and $3d_{5/2}$ by u, u′, u″ and u‴ in Fig. 12 [31,43]. Apparent u′ and v′ peaks assigned to Ce^{3+} are observed over the TWCs aged, while the peak intensity for u‴ assigned to Ce^{4+} decreased. No u′ and v′ peaks were observed over the fresh TWCs. The transformation of Ce^{4+} to Ce^{3+}, probably caused by the formation of $Ce_2(SO_4)_3$ and $CePO_4$ by S and P discussed in Fig. 8 can be anticipated in line with the results by the XANES analysis for Ce L_3-edge of Ce^{3+} on the catalyst surface.

Table 4 shows the results of OSC and OSCC determined over the fresh and aged TWCs employed. OSC representing the oxygen mobility of TWC gradually decreases as the catalyst mileage increases. It may probably cause the gradual deactivation of TWC, determined by ST. The decrease of OSCC, the amounts of total oxygen stored onto CZ lattice, may also degrade CZ as well.

Table 4
OSC and OSCC of the fresh and aged TWCs over the Pd7 and Pd10 TWCs.

Samples	OSC (μmol/g_{cat})	OSCC (μmol/g_{cat})
Pd7-fresh	125	221
Pd7-21,000	112	146
Pd7-55,000	101	132
Pd10-fresh	148	315
Pd10-41,000	121	141
Pd10-98,000	90	128

However, the changing degree of OSCC is not clearly proportional to the catalyst mileage, compared to that of OSC. It simply reflects that the critical decrease of OSCC of CZ occurs in the initial period of the catalyst aging [9], while the alteration of OSC, oxygen mobility proportionally depends on the catalyst mileage.

4. Discussion

4.1. Phase transformation of Ce

The role of Ce, particularly as an OSC promoter is indeed significant for the deactivation of TWC as extensively discussed. The state of Ce existing on the surface of TWC in the form of CZ can be altered by two causes, catalyst sintering as well as poisoning under the practical automotive exhaust condition [5,33–35]. In order to elucidate two distinct oxidation activities of CO and C_3H_6 by ST as observed, the state of Ce has been systematically characterized.

From the XRD results of the fresh and aged TWCs as shown in Fig. 8, the separation of CZ ($Ce_xZr_{(1-x)}O_2$) into two phases, CeO_2 and ZrO_2 leading the growths of these particle sizes on the surface of TWC is apparent as the catalyst mileage increases. Also, a shoulder between the peaks of CeO_2 and ZrO_2 indicates the existence of CZ on the catalyst surface. This may be direct evidence for the phase separations of CZ contained in TWC toward CeO_2 and ZrO_2 as the catalyst deactivation proceeds [36]. The deactivation of the OSC performance of TWC can be anticipated due to the exposure of the catalyst contained in WCC to the high temperature environment [44]. In addition, the phase separation of CZ begins even in the initial period of catalyst field-aging mileage as reflected in the XRD results over Pd7-21000.

Moreover, the formation of $Ce_2(SO_4)_3$ and $CePO_4$, regarded as one of the major deactivation agents altering the valence transition of Ce, has been identified on the catalyst surface as the mileage increases. Since they are stable chemical compounds, the re-transition of Ce valance from tri- to tetra-state again may be hardly

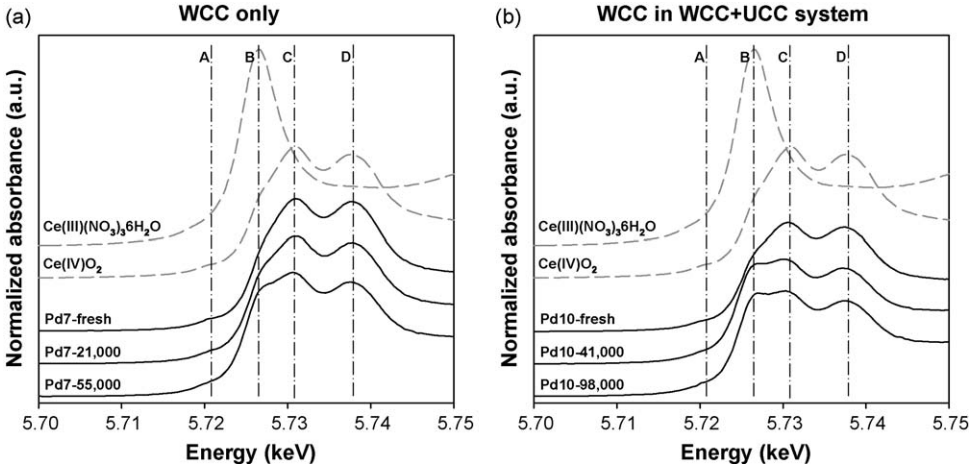

Fig. 10. Ce L_{III}-edge XANES spectra over the fresh and aged Pd TWCs; (a) Pd7 and (b) Pd10 TWCs.

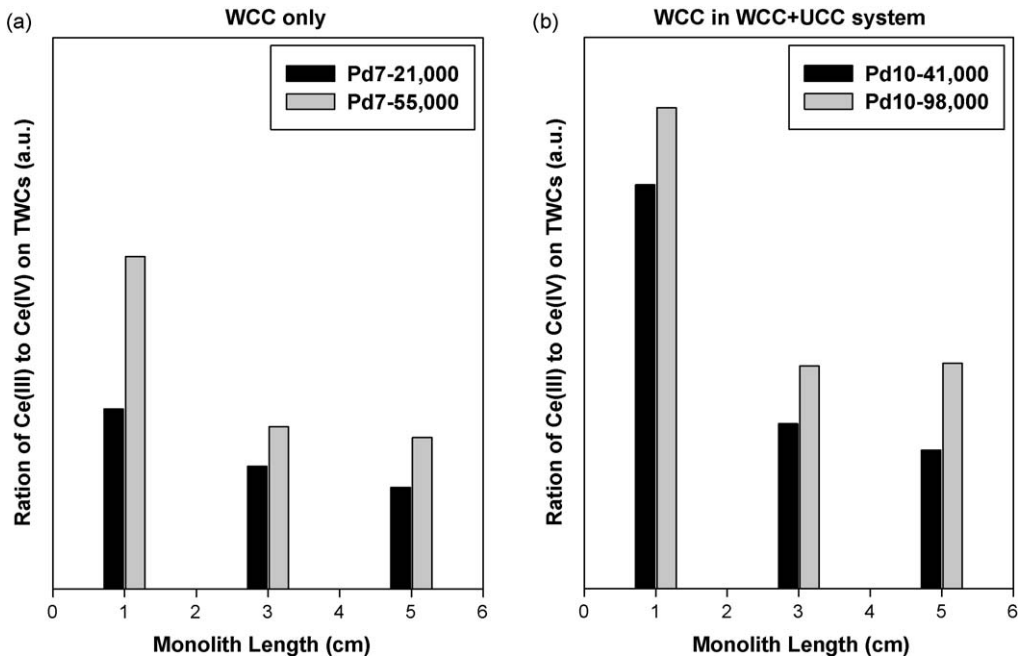

Fig. 11. Relative amount of Ce^{3+} formed on CZ by the deconvolution of XANES peaks using the arctangent and Gaussian functions; (a) Pd7 and (b) Pd10 TWCs.

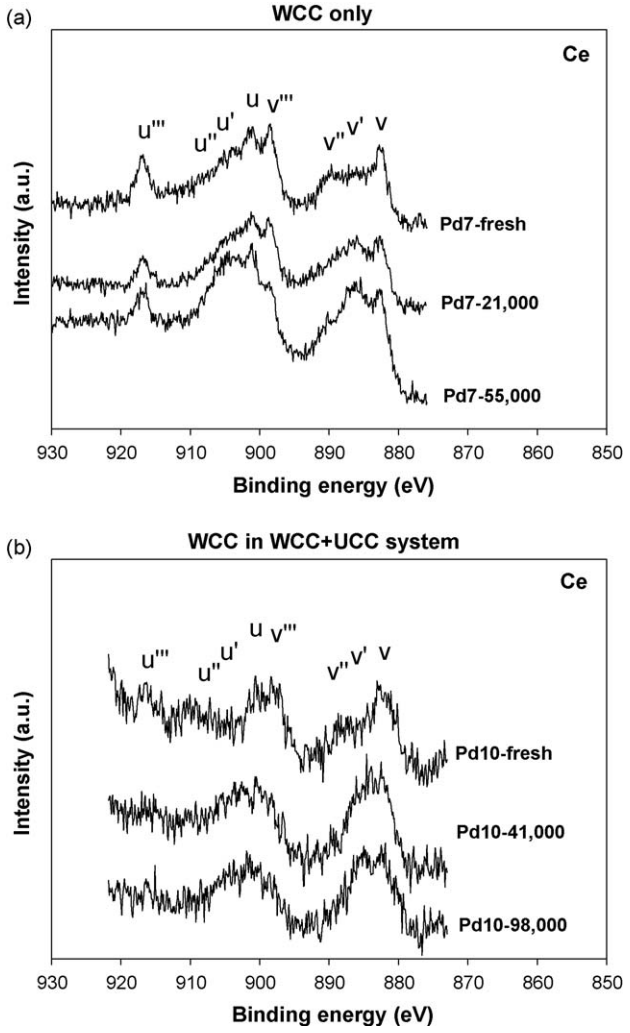

Fig. 12. XPS spectra (Ce 3d) of the fresh and aged Pd TWCs; (a) Pd7 and (b) Pd10 TWCs.

expected. Indeed, Larese et al. [34] reported that $CePO_4$ was stable even at 1173 K, whereas the S compounds formed on Pd/Ce catalyst were reduced to H_2S at 723 K under reducing condition as discussed by Luo et al. [5].

The sequential H_2 TPR profiles over the fresh and aged TWCs for WCC only and WCC + UCC systems conducted in the present study showed the decomposition of S compounds into H_2S from 900 K as depicted in Fig. 9. By the re-oxidation and reduction of the Pd7-55,000 pre-reduced at 1173 K for 10 min, the advent of a new hydrogen consumption peak by the reduction of CeO_2 has been observed at 723 K. The S compounds, mainly $Ce_2(SO_4)_3$, can be easily decomposed under rich condition of the gasoline engine exhaust [5,35], while $CePO_4$ is thermally stable even at 1173 K [34]. It may explain the variation of the amounts of S deposited onto the surface of TWC, regardless of the catalyst Pd content and mileage as shown in Fig. 7. Thus, the stable $CePO_4$ formed is the primary deactivation precursor over TWCs customer-aged. Indeed, as determined by ICP-OES in Fig. 7, the large amount of P deposited onto TWC, eventually forming $CePO_4$ on the catalyst surface, increases as the catalyst mileages increase [7,34].

The state of Ce was also identified by XANES analysis of Ce L_3-edge over the fresh and aged TWCs, as shown in Fig. 10. Ce^{3+} may exist in forms of the deactivating agents, $CePO_4$ and $Ce_2(SO_4)_3{\cdot}5H_2O$ on the catalyst surface by the reaction of P or S deposited onto the catalyst surface with CeO_2 split from CZ by phase separation. As determined by the deconvolution of the XANES peaks in Fig. 11, the relative amount of Ce^{3+} contained in CZ increases as the aging mileage increases. It is also consistent with the increase of the amounts of P deposited onto the surface of TWCs confirmed by ICP-OES in Fig. 7. No correlation of the amount of S deposited to that of Ce^{3+}, however, was observed. The XPS analysis in the Ce 3d region of the catalysts also identifies the existence of Ce^{3+} on the catalyst surface with respect to the catalyst mileages as reflected in Fig. 12.

4.2. The alteration of Pd-Ce interaction

Since the variation of the chemical state of Ce and Pd can be another evidence for the degradation of the OSC attributed to the

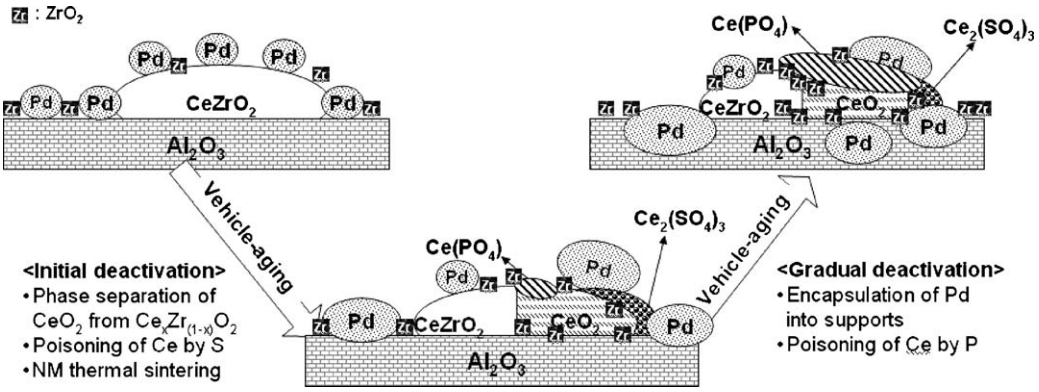

Fig. 13. Schematic deactivation process of Pd TWCs containing CZ.

interaction of Pd-Ce sharing O atom [45], it may also clarify the gradual deactivation of TWC with respect to the catalyst mileage determined by ST, not by st-ST and LOT.

The shift of the binding energy of Pd by XPS in the region of Pd 3d from 336.3 to 334.7 eV may reveal the sintering of Pd on the surface of TWC with respect to the catalyst mileage as shown in Fig. 5. Indeed, partially oxidized Pd particles exist on the surface of the fresh TWC by the interaction of Pd-Ce [46,47]. However, as the deactivation of TWC proceeds with respect to the catalyst mileage, the alteration of the state of Ce contained in CZ and the formation of the larger Pd particle agglomerated by sintering of Pd particles occur simultaneously, leading to the degradation of the interaction of Pd with Ce [45–47].

The gradual loss of metallic Pd from the catalyst surface as observed by the decrease of the intensity of the XPS peak at 334.7 eV, further weakens the interaction of Pd-Ce. Note that the Pd existing within about 5 nm in the vertical depth from the catalyst surface can be identified by XPS analysis [48]. The peak intensity of Pd7 included in WCC only system at 334.7 eV gradually decreased as the catalyst mileage increased. A considerable amount of metallic Pd still exists on the surface of Pd7-55,000. However, a negligible peak for Pd at 334.7 eV over Pd10-98,000 possessing the highest aging mileage among the samples examined in the present study was observed, while a shoulder peak can be observed over Pd10-41,000. It may reveal the gradual encapsulation of Pd into the layer of the washcoats of monolith, resulting in the decrease of the number of the active reaction sites and the alteration of the interaction of Pd with CZ with respect to the catalyst mileages [49,50]. Note that the deconvolution of the peaks could hardly be conducted for quantifying the amount of Pd on the catalyst surface remaining, mainly attributed to the overlapping of the XPS peaks of the chemical elements including Pd, Zr and Ca contained in TWC [50].

The overall deactivation scheme of Pd-based TWC included in the front brick of WCC is summarized in Fig. 13. Two steps for the deactivation of TWC, initial and gradual, are systematically illustrated. In the initial stage of the catalyst aging, the activity of the TWCs apparently decreases due to the sintering of Pd, the phase separation of CZ and the poisoning by P and S contained in the exhaust gas from a gasoline driven engine. They alter the redox property, OSC and OSCC, of TWCs. The catalyst is then gradually deactivated by the continuous poisoning of P and the encapsulation of Pd into the catalytic layer of the monolith. They will further reduce the redox property of CZ and weaken the interaction of Pd to Ce, causing the degradation of OSC of TWC. Another cause attributed to the spillover and back-spillover of oxygen between Pd and ceria may not be ignored, since they can also be changed by the alteration of Pd-Ce interaction and the encapsulation of Pd [51–53].

5. Conclusions

The deactivation of the oxidation activities over TWCs was examined with respect to the catalyst field mileage by three test modes: ST, st-ST and LOT. No change of the oxidation activity of C_3H_6 at 673 K was observed, regardless of the catalyst mileage. This is probably due to the dominant oxidative capability of Pd toward hydrocarbons at 673 K. However, the activity of CO gradually decreased with respect to the catalyst mileage by ST. The catalyst deactivation is mainly due to the sintering of NM and degradation of OSC. Although the sintering of NM might be responsible for the initial deactivation of TWCs, the gradual deactivation of the oxidation reactions could be hardly explained by sintering itself. As the catalyst deactivation proceeds, the OSC of TWC is simultaneously decreased, mainly due to the degradation of CZ and weakness of Pd-Ce interaction. The degradation of CZ has been attributed to the phase separation of CeO_2 from $Ce_xZr_{(1-x)}O_2$ in the initial period of the catalyst aging and the gradual transformation of Ce^{+4} to Ce^{3+}. The OSC of TWC is further decreased by the weakness of the Pd-Ce interaction through the sintering of Pd in the initial period of the catalyst aging and the gradual encapsulation of Pd with respect to the catalyst mileages. Finally, the ST is essential to appropriately determine the catalyst deactivation of TWC.

Acknowledgments

This work is part of the project "Development of Partial Zero Emission Technology for Future Vehicle" funded by Ministry of Knowledge and Economy and we are grateful for its financial support. Another financial support of this work was provided by the National Research Laboratory Program (ROA-2007-000-20050-0) of the Korea Science and Engineering Foundation.

References

[1] R.M. Heck, R.J. Farrauto, S.T. Gulati, Commercial Technology, 2nd ed., John Wiley & Sons, Inc., New York, 2002.
[2] J. Kašpar, P. Fornasiero, N. Hickey, Catal. Today 77 (2003) 419.
[3] D.R. Liu, J.S. Park, Appl. Catal. B: Environ. 2 (1993) 49.
[4] C. Larese, F.C. Galisteo, M.L. Granados, R. Mariscal, J.L.G. Fierro, P.S. Lambrou, A.M. Efstathiou, J. Catal. 226 (2004) 443.
[5] T. Luo, J.M. Vohs, R.J. Gorte, J. Catal. 210 (2002) 397.
[6] P.S. Lambrou, P.G. Savva, J.L.G. Fierro, A.M. Efstathiou, Appl. Catal. B: Environ. 76 (2007) 375.
[7] M.L. Granados, F.C. Galisteo, P.S. Lambrou, R. Mariscal, J. Sanz, I. Sobrados, J.L.G. Fierro, A.M. Efstathiou, J. Catal. 239 (2006) 410.
[8] S.Y. Christou, H. Birgersson, J.L.G. Fierro, A.M. Efstathiou, Environ. Sci. Technol. 40 (2006) 2030.
[9] M.L. Granados, C. Larese, F.C. Galisteo, R. Mariscal, J.L.G. Fierro, R. Fernández-Ruíz, R. Sanguino, M. Luna, Catal. Today 107–108 (2005) 77.
[10] J.R. González-Velasco, J.A. Botas, R. Ferret, M.P. González-Marcos, J.-L. Marc, M.A. Gutiérrez-Ortiz, Catal. Today 59 (2000) 395.

[11] J.P. Cuif, S. Deutsch, M. Marczi, H.W. Jen, G.W. Graham, W. Chun, R.W. McCabe, SAE 980668 (1998).
[12] H. Muraki, G. Zhang, Catal. Today 63 (2000) 337.
[13] R. Dictor, S. Roberts, J. Phys. Chem. 93 (1989) 5846.
[14] S.Y. Christou, A.M. Efstathiou, Top. Catal. 42–43 (2007) 351.
[15] G.W. Graham, H.-W. Jen, W. Chun, R.W. McCabe, J. Catal. 182 (1999) 228.
[16] Y. Song, J. Jang, G. Yeo, J. Lee, SAE (1998), 980666.
[17] J.H. Baik, H.J. Kwon, Y.T. Kwon, I.-S. Nam, S.H. Oh, Top. Catal. 42–43 (2007) 337.
[18] D.S. Lafyatis, C.J. Bennett, M.A. Hales, D. Morris, J.P. Cox, R.R. Rajaram, SAE 1999-01-0309 (1999).
[19] G.C. Koltsakis, A.M. Stamatelos, Prog. Energy Combust. Sci. 23 (1997) 1.
[20] J.R. González-Velasco, J.A. Botas, J.A. González-Marcos, M.A. Gutiérez-Ortiz, Appl. Catal. B: Environ. 12 (1997) 61.
[21] J.G. Nunan, G.W. Denison, W.B. Williamson, M.G. Henk, SAE, PT-123 (2006) 83.
[22] H.J. Kwon, J.H. Baik, Y.T. Kwon, I.-S. Nam, S.H. Oh, Chem. Eng. J. 141 (2008) 194.
[23] J.H.B.J. Hoebink, R.A. Gemert, J.A.A. Tillaart, G.B. Marin, Chem. Eng. Sci. 55 (2000) 1573.
[24] R. Strobel, F. Krumeich, W.J. Stark, S.E. Pratsinis, A. Baiker, J. Catal. 222 (2004) 307.
[25] H.C. Yao, Y.F.Y. Yao, J. Catal. 86 (1984) 254.
[26] J.W. Choung, I.-S. Nam, Appl. Catal. A: Gen. 312 (2006) 165.
[27] Z. Hu, C.Z. Wan, Y.K. Lui, J. Dettling, J.J. Steger, Catal. Today 30 (1996) 83.
[28] H. Shinjoh, H. Muraki, Y. Fujitani, Appl. Catal. 49 (1989) 195.
[29] M. Fernández-García, A. Iglesias-Juez, A. Martínez-Arias, A.B. Hungría, J.A. Anderson, J.C. Conesa, J. Soria, J. Catal. 221 (2004) 594.
[30] P.J. Schmitz, K. Otto, J.E. deVries, Appl. Catal. A: Gen. 92 (1992) 59.
[31] H. He, H.X. Dai, C.T. Au, Catal. Today 90 (2004) 245.
[32] H. Birgersson, M. Boutonnet, F. Klingstedt, D.Y. Murzin, P. Stefanov, A. Naydenov, Appl. Catal. B: Environ. 65 (2006) 93.
[33] K. Kenevey, F. Valdivieso, M. Soustelle, M. Pijolat, Appl. Catal. B: Environ. 29 (2001) 93.
[34] C. Larese, F.C. Galisteo, M.L. Granados, R.M. Lŏpez, J.L.G. Fierro, P.S. Lambrou, A.M. Efstathiou, Appl. Catal. B 48 (2004) 113.
[35] C. Larese, M. López Granados, F. Cabello Galisteo, R. Mariscal, J.L.G. Fierro, Appl. Catal. B: Environ. 62 (2006) 132.
[36] C.W. Chou, S.J. Chu, H.J. Chiang, C.Y. Huang, C.J. Lee, S.R. Sheen, P.P. Perng, C.T. Yeh, J. Phys. Chem. B 105 (2001) 9113.
[37] G. Chen, W.-T. Chou, C.-t. Yeh, Appl. Catal. 8 (1983) 389.
[38] H.-W. Jen, G.W. Graham, W. Chun, R.W. McCabe, J.-P. Cuif, S.E. Deutsch, O. Touret, Catal. Today 50 (1999) 309.
[39] B. Scheffer, P. Molhoek, J.A. Moulijn, Appl. Catal. 46 (1989) 11.
[40] H.N. Rabinowitz, S.J. Tauster, R.M. Heck, Appl. Catal. A: Gen. 212 (2001) 215.
[41] P. Fornasiero, J. Kašpar, M. Graziani, Appl. Catal. B: Environ. 22 (1999) L11.
[42] A. Norman, V. Perrichon, A. Bensaddik, S. Lemaux, H. Bitter, D. Koningsberger, Top. Catal. 16–17 (2001) 363.
[43] J.Z. Shyu, K. Otto, W.L.H. Watkins, G.W. Graham, R.K. Belitz, H.S. Gandhi, J. Catal. 114 (1988) 23.
[44] C. Bozo, F. Gaillard, N. Guilhaume, Appl. Catal. A: Gen. 220 (2001) 69.
[45] C.E. Gigola, M.S. Moreno, I. Costilla, M.D. Sánchez, Appl. Surf. Sci. 254 (2007) 325.
[46] X. Wu, L. Xu, D. Weng, Appl. Surf. Sci. 221 (2004) 375.
[47] Y. Nagai, T. Hirabayashi, K. Dohmae, N. Takagi, T. Minami, H. Shinjoh, S. Matsumoto, J. Catal. 242 (2006) 103.
[48] J.W. Niemantsverdriet, Spectroscopy in Catalysis, An Introduction, 2nd ed., Wiley-VCH, 2000 Completely Revised Edition.
[49] J. Fan, X. Wu, X. Wu, Q. Liang, R. Ran, D. Weng, Appl. Catal. B: Environ. 81 (2008) 38.
[50] U. Lassi, R. Polvinen, S. Suhonen, K. Kallinen, A. Savimäki, M. Härkönen, M. Valden, R.L. Keiski, Appl. Catal. A: Gen. 263 (2004) 241.
[51] M. Zhao, M. Shen, J. Wang, W. Wang, Ind. Eng. Chem. Res. 46 (2007) 7883.
[52] N. Hickey, P. Fornasiero, J. Káspar, J.M. Gatica, S. Bernal, J. Catal. 200 (2001) 181.
[53] P.S. Lambrou, C.N. Costa, S.Y. Christou, A.M. Efstathiou, Appl. Catal. B: Environ. 54 (2004) 237.